Structural characteristics of extracellular polymeric substances (EPS) in membrane bioreactor and their adsorptive fouling

Xinying Su and Zhigang Zhang

ABSTRACT

The soluble (S), loosely bound (LB) and tightly bound (TB) extracellular polymeric substances (EPS) were extracted from sludge flocs of a membrane bioreactor to evaluate their characteristics and adsorptive fouling. The degrees of adsorptive fouling by the EPS fractions were in the order S-EPS < TB-EPS < LB-EPS. The images of atomic force microscopy showed the membrane fouled by LB-EPS was rougher than that fouled by the other fractions. The adsorbed EPS layer, which was sensed by quartz crystal microbalance with dissipation, was found to be more rigid and compact for LB-EPS, compared with the other EPS fractions. The excitation–emission matrix and Fourier transform infrared techniques were also used to characterize the individual EPS fractions. Compared with S-EPS and TB-EPS, the LB-EPS contained a larger amount of aromatic protein and less carbohydrates and lipids, exhibiting characteristics of greater aromaticity and hydrophobicity. These characteristics should be responsible for more severe fouling, and the stiffer and more compact structure of the adsorbed layer.

Key words | adsorptive fouling, loosely bound EPS (LB-EPS), membrane bioreactor (MBR), membrane fouling

Xinying Su (corresponding author)
Department of Environmental Engineering,
School of Food Engineering,
Harbin University of Commerce,
Harbin 150076,
China
E-mail: *suxinyinghit@163.com*

Zhigang Zhang
Science and Technology on Underwater Acoustic Laboratory, College of Underwater Acoustic Engineering,
Harbin Engineering University,
Harbin 150001,
China

INTRODUCTION

The membrane bioreactor (MBR) is a promising wastewater treatment technology which has some advantages over conventional activated sludge systems, including stable and high effluent quality, ease of operation, small footprint, and absolute removal of bacteria (Kimura *et al.* 2008; Deng *et al.* 2016; Meng *et al.* 2017). However, membrane fouling remains the most serious problem for widespread application of MBR technology.

Extracellular polymeric substances (EPS), a complex high-molecular-weight mixture of polymers produced by active secretion, shedding of cell surface material or cell lysis, have been considered as the major cause of membrane fouling in MBRs (Drews *et al.* 2006; Boltz *et al.* 2017). Chemically, EPS contain a lot of complex organic matter, such as proteins, polysaccharides, humic substances, nucleic acids, organic acids, amino acids, and extracellular enzymes (Le-Clech *et al.* 2006). EPS are the construction materials for microbial aggregates such as sludge flocs, which can be further classified into three categories: soluble EPS (S-EPS), loosely bound EPS (LB-EPS) and tightly bound EPS (TB-EPS) based on the extraction methodology (Yu *et al.* 2008). The characteristics and contents of the main components in EPS are found to affect the properties of microbial aggregates crucially, such as surface characteristics, adsorption ability, stability, flocculating behavior, settleability, compressibility, dewaterability etc. (Sheng *et al.* 2010). So far, most of the previous studies have focused on the characteristics and fouling potential of EPS and the influence of operating conditions on EPS production and characteristics (Kim *et al.* 2006; Malamis & Andreadakis 2009; Sun *et al.* 2016). It has been reported that S-EPS contribute 26–52% of membrane fouling for microfiltration or ultrafiltration membranes in MBRs (Yang *et al.* 2011; Guo *et al.* 2012). Furthermore, filtration resistance has been found to correlate with the chemical oxygen demand (COD) in the sludge water (i.e. S-EPS), but not to the bound EPS (Rojas *et al.* 2005), whereas, it was reported that the filterability of sludge decreased and the specific cake resistance became higher as the amount of bound EPS increased (Nagaoka *et al.* 1996). Furthermore, lots of methods and technologies have been used to detect the characteristics and fouling potential of EPS. For example,

doi: 10.2166/wst.2018.033

Fourier transform infrared (FTIR) spectroscopy is used for analyzing the chemical functional groups of EPS and the membrane (An *et al.* 2009). Three-dimensional excitation–emission matrix (EEM) fluorescence spectroscopy is used to identify aromatic protein-like substances, fulvic acid-like materials, soluble microbial byproduct-like material and humic acid-like substance in EPS (Wang *et al.* 2009b). Atomic force microscopy (AFM) is used for measuring the surface roughness, which may influence the fouling degree of the membrane surface (Shen *et al.* 2010). Recently, quartz crystal microbalance with dissipation (QCM-D) has been used to analyze the adherence and viscoelastic properties of EPS and the structural properties of adsorbed layers (Sweity *et al.* 2011; Motsa *et al.* 2015; Wang *et al.* 2016).

In terms of fouling mechanisms in MBRs, fouling behavior over time is generally characterized by a three-phase evolution (Le-Clech *et al.* 2006; Zhang *et al.* 2006; Drews 2010). Phase 1 is conditioning fouling; strong interactions between the membrane surface and the EPS present in the mixed liquor are probably responsible for the initial stage of fouling. Phase 2 is a prolonged period of slow transmembrane pressure (TMP) rise, which might be due to the accumulation of organic macromolecules, either deposited from the bulk liquor or produced by microorganisms on the membrane surface. Phase 3 is a sudden rise in TMP (TMP jump), mainly because the overall permeate productivity redistributes to the less-fouled membrane areas or pores, leading to local flux increases exceeding the critical flux. Phase 1 has not been observed or described as such until recently, but may be a key aspect of fouling creation in MBRs (Le-Clech *et al.* 2006). Considering the contribution of relative hydraulic resistance, the initial adsorption has been reported to account for 20–2,000% of the clean membrane resistance(Ognier *et al.* 2002). Furthermore, the interaction between EPS and the membrane surface may play a significant role in modifying surface characteristics and creating suitable conditions for biomass attachment (Zhang *et al.* 2008), eventually colonizing the separation surface and contributing to phase 2. However, the adsorptive behaviors of TB-EPS, LB-EPS and S-EPS extracted from activated sludge in MBRs have not been studied in the literature. A detailed comparison of the EPS fractions extracted from activated sludge will help in understanding membrane fouling better.

Therefore, the purpose of this study is to investigate the adsorptive behaviors of S-EPS, LB-EPS and TB-EPS extracted from activated sludge in MBR. The contribution of individual EPS fractions (hereafter referred to as 'individial EPS') to membrane adsorptive fouling was identified. The adsorption and viscoelastic properties of individual EPS were evaluated. Furthermore, the characteristics of individual EPS were also determined to understand the adsorptive behaviors of different EPS fractions.

MATERIALS AND METHODS

Membrane bioreactor system

A 150 L MBR (as schematically shown in Figure S1, available with the online version of this paper) was installed with three submerged hollow fiber polyvinylidene fluoride microfiltration (MF) membrane modules (Tianjin Motian Membrane Engineering and Technology Co. Ltd, China). The MF membrane module is characterized with a nominal pore size of 0.2 μm and a filtration area of 1 m^2.

The bioreactor was fed with synthetic wastewater from a wastewater tank; a liquid level control was used to control the water level in the bioreactor. The effluent was controlled by a peristaltic pump. Aeration was provided continuously underneath the membrane modules so as to control membrane fouling and supply air to the biomass. The dissolved oxygen (DO) was monitored with a portable on-line DO meter (WTW inoLab Oxi level 2) and aeration rate was adjusted through the air flow meter. Flux, temperature, pH, and TMP were regularly monitored. The MBR was operated under constant flux of 8 L/(m^2 h) with a suction cycle of 8 min followed by 2 min relaxation, which was controlled by a peristaltic pump. The sludge retention time was 30 days and the hydraulic retention time was 10 h. The fouling rate was evaluated by the change of TMP. When the TMP reached 45 kPa, chemical cleaning (soaking for 2–8 h in 0.5% sodium hypochlorite solution) was provided.

During the experiments, the synthetic wastewater used for this study mainly contained glucose and starch, carbamide, and KH_2PO_4 as the sources of carbon, nitrogen, and phosphorus, respectively. The trace metals required for biomass growth were added periodically. The composition of the synthetic wastewater was as follows: 176 mg of glucose, 176 mg of starch, 63.3 mg of carbamide, 252.7 mg of sodium bicarbonate, 15.4 mg of KH_2PO_4, 19.6 mg of K_2HPO_4, 51 mg of $MgSO_4{\cdot}7H_2O$ and 12.5 mg of $CaCl_2$ per litre. Trace metals were added twice a week and the composition was as follows: 0.13 mg of $ZnCl_2$, 17.48 mg of $FeSO_4{\cdot}7H_2O$, 0.27 mg of $Pb(NO_3)_2$ and 0.13 mg of $MnSO_4{\cdot}4H_2O$ per litre.

Prior to the experiments, the MBR was operated for over 3 months. The food-to-microorganism ratio was 0.13 kg-COD kg-MLSS^{-1} d^{-1} and the mixed liquid suspended

solids (MLSS) concentration was 9,000 ± 600 mg L^{-1}. The soluble COD was 48 ± 10 mg L^{-1}.

Extraction and analysis of EPS

The EPS from the sludge sample were extracted according to a two-step heat extraction method (Li & Yang 2007). The mixed liquor (50 mL) of activated sludge was centrifuged at 4,000 *g* for 5 min. The supernatant was defined as the S-EPS. The sludge pellet was resuspended with 0.85% NaCl solution to 50 mL at 50 °C and then immediately sheared by a vortex mixer for 1 min. The sludge suspension was then centrifuged at 4,000 *g* for 10 min, and the organic matter in the supernatant was regarded as the readily extractable EPS or the LB-EPS of the biomass. For further TB-EPS extraction, the sludge pellet was resuspended in 0.85% NaCl solution to its original volume of 50 mL. The sludge suspension was heated at 80 °C in a water bath for 30 min and then it was centrifuged at 4,000 *g* for 15 min. The organic material in the supernatant was regarded as the TB-EPS. The EPS solution collected was filtered with a 0.45 μm membrane filter and dialyzed through a dialysis membrane for a few days to remove salts.

Adsorptive fouling experiments

These experiments were performed in a stirred dead-end membrane filtration cell with approximately 12.56 cm^2 membrane area. The pure water flux of a fresh flat sheet membrane (nominal pore size: 0.22 μm) was measured with temperature of 20 ± 2 °C. The EPS solution was contacted with the surface of the membrane for a pre-determined period. Then the membrane was taken out, briefly rinsed with pure water for approximately 5 min and the pure water flux of the membrane was measured again. The flux reduction of pure water flux was calculated by comparing the pure water flux before and after the EPS solution adsorption as follows:

$$R(\%) = \frac{F_b - F_a}{F_b} \times 100\% \quad (1)$$

where R was the flux reduction of pure water (%); F_b and F_a were the pure water flux before and after adsorption (L m^{-1} h^{-1}), respectively[1].

QCM-D analysis

QCM-D is a powerful acoustic technique with nanogram sensitivity, which can measure the mass and structural changes that occur on the surface of a quartz sensor in real-time (Sweity *et al.* 2011; Motsa *et al.* 2015; Wang *et al.* 2016). In this study, QCM-D was used for analyses of adherence and viscoelastic properties of individual EPS. The QCM-D monitoring measurements were performed with AT-cut quartz crystals mounted in an E4 system (Q-sense AB, Gothenburg, Sweden). The gold-coated crystals (Q-Sense AB), with a fundamental resonant frequency of around 5 MHz, were used in this study. Before each measurement, the gold-coated sensors were soaked in a 5% ethylenediaminetetraacetic acid (EDTA) solution for 30 min, rinsed thoroughly with double distilled water, dried with pure nitrogen gas, and treated for 10 min in a UV/O_3 chamber. All QCM-D experiments were performed under flow-through conditions using a digital peristaltic pump (IsmaTec, IDEX) operating in sucking mode at 20 °C. The pump tubing was connected to a glass vial containing the studied solutions that were injected into the sensor crystal chamber at 0.03 mL min^{-1} (Ying *et al.* 2010).

A commercial software program (Q-Tools, Q-Sense AB, Gothenburg, Sweden) developed for QCM-D was used for the calculations. In the Voigt modeling, bulk density and bulk viscosity values of 1.0 g cm^{-3} and 0.001 Pa·s, respectively, were used for all fits.

Analytical methods

Standard analytical methods were adopted for measurements of total suspended solids and volatile suspended solids in the bioreactor and sludge volume index (APHA 1995). The dissolved organic carbon (DOC) was analyzed using a total organic carbon (TOC) analyzer (TOC-VCPH/TOC-5000, Shimadzu, Japan). Ultraviolent (UV) absorbance of samples was measured with a UV–visible spectrophotometer (UV-2550, Shimadzu, Japan) at 254 nm. Specific ultraviolet light absorbance (SUVA) was calculated as UV-254/DOC, which characterized aromaticity of the individual EPS (Wei *et al.* 2011).

The EEM spectra were measured using a fluorescence spectrophotometer (FP-6500 spectrophotometer, Jasco, Japan). The EEM spectra were obtained by scanning the sample over excitation wavelengths from 220 to 450 nm with 5 nm steps and emission wavelengths from 220 to 600 nm with 1 nm steps. The software Origin 7.0 (OriginLab Inc., USA) was employed to process the EEM data.

Functional group characteristics of the LB-EPS, TB-EPS and S-EPS were characterized by an FTIR spectrometer (Perkin-Elmer Spectrum One B, Perkin-Elmer, USA). Lyophilized dried powders (2–5 mg) were pressed with 200 mg

KBr (FTIR grade) and measured immediately after preparation under ambient conditions. Spectra were baseline corrected and normalized to 1.0 for the purpose of comparison.

AFM (Veeco, Santa Barbara, CA, USA) was performed in tapping mode to describe foulant layer morphology in terms of membrane surface topography and pore distribution. Membrane sheets were dried at 50 °C for 48 h. The Nanoscope control software (Version 5.30r3sr3) was used for image acquisition. Surface roughness is an important parameter of fouling degree and the values of mean roughness (Ra) were obtained based on 10.0 μm × 10.0 μm scan area.

For QCM-D analysis and EEM spectra analysis, each fraction was diluted to the same TOC level (TOC = 10 mg L^{-1}). All the above analyses were conducted in triplicate.

RESULTS AND DISCUSSION

The adsorption behaviors of individual EPS

Adsorptive fouling of individual EPS

The tests of adsorption for individual EPS using the stirred cells were conducted for the three different EPS components to investigate the effect of the individual EPS on membrane fouling.

The variations of pure water fluxes with time for individual EPS samples are shown in Figure 1. All pure water fluxes of membranes fouled by individual EPS decreased with the adsorption time, suggesting that the adsorption of different EPS samples led to the fouling. It was also noted that the decrement rate of membrane flux for individual EPS showed the trend of LB-EPS > TB-EPS > S-EPS, implying the LB-EPS led to more significant fouling compared with TB-EPS and S-EPS. In comparison with the initial flux of fresh membranes, the pure water fluxes of membranes fouled by S-EPS resulted in 17.7%, 24.8% and 29.9% decrement after 1 h, 2 h and 3 h adsorption, respectively, and the corresponding profiles for 4 h and 5 h adsorption indicated a leveling off. In contrast, the decreases of pure water fluxes for membranes fouled by TB-EPS were 19.6%, 30.9% and 37.6% after 1 h, 2 h and 3 h adsorption, respectively; it was noted that pure water fluxes had little change as the experiment progressed from 4 h to 5 h. For membranes fouled by LB-EPS, the decrease of pure water fluxes were 29.1%, 39.4%, 45.7%, 47.7% and 48.6% after 1 h, 2 h, 3 h, 4 h and 5 h adsorption, respectively. From Figure 1, it was also noted that at 4 h EPS adsorption was almost saturated. Adsorptive fouling is the first phase of the MBR fouling, which may modify the surface characteristics of membranes, eventually providing conditions suitable for biomass attachment and cake deposition (Su *et al.* 2014). EPS are usually considered as the major cause of membrane fouling in MBRs. These results suggested that significant adsorptive fouling only occurred in the initial hours and LB-EPS showed the most serious adsorptive fouling.

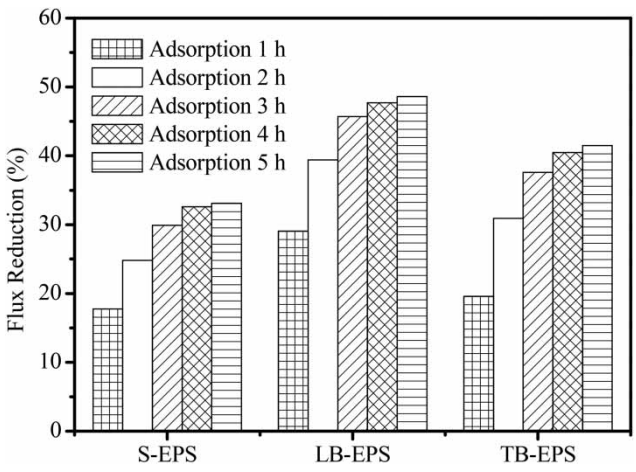

Figure 1 | Variation of pure water flux.

AFM observation

The AFM images of fresh and fouled membranes surfaces (5 h adsorption was selected) are presented in Figure 2. Changes in surface morphology were observed for all the samples. Fresh membrane was relatively smoother, while the fouled membrane surface was covered with foulants. The Ra of fresh membrane was 127.42 nm. For the membrane fouled by S-EPS, LB-EPS and TB-EPS, the Ra increased to 136.27 nm, 200.07 nm and 171.57 nm after 5 h adsorption, respectively. Compared with the fresh membrane, the increase in Ra of fouled membrane might be attributed to the surface enrichment of large molecules caused by adsorption of EPS. Moreover, the Ra of membrane fouled by TB-EPS was lower than that by LB-EPS, which could be attributed to the result of the deposition of more small molecules on the ridge-and-valley structure of the membrane and in pores for membrane fouled by TB-EPS. Rougher and more hydrophobic membranes have a higher tendency for fouling (Herzberg *et al.* 2009). These results further confirmed the LB-EPS showed a stronger potential for

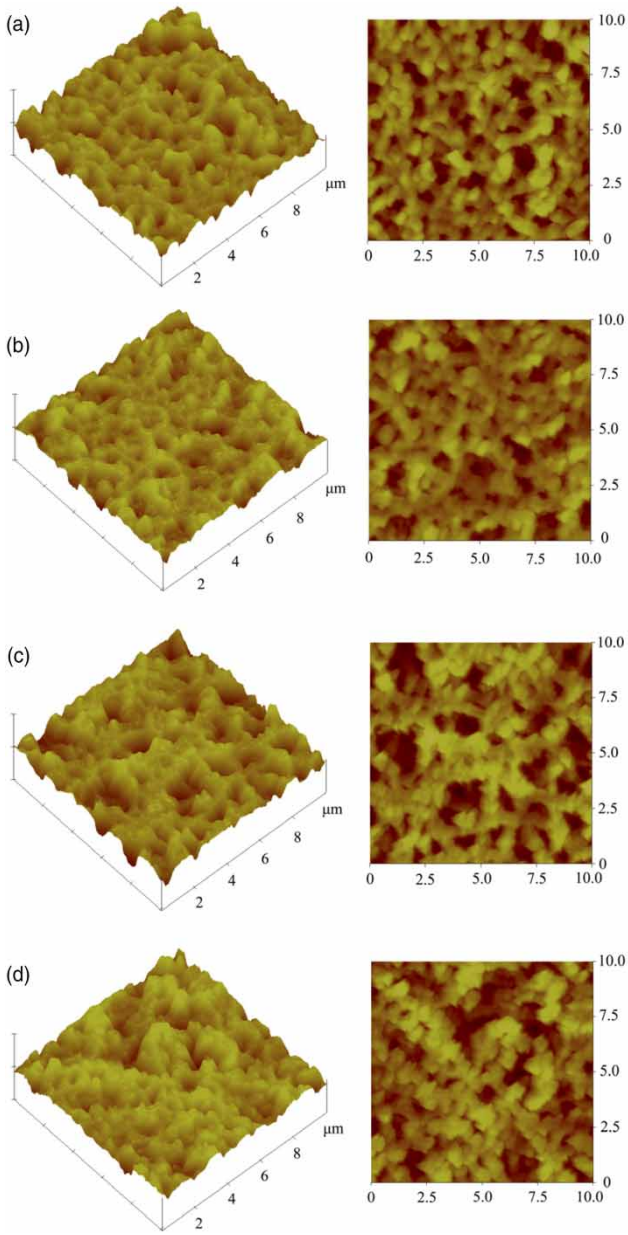

Figure 2 | AFM images of fresh and fouled membrane surfaces: (a) fresh membrane; (b) membrane fouled by S-EPS; (c) membrane fouled by LB-EPS; (d) membrane fouled by TB-EPS.

adsorptive fouling than S-EPS and TB-EPS. And the surface of membrane fouled by LB-EPS was rougher.

Adsorption and viscoelastic properties of individual EPS

EPS viscoelasticity is strongly related to the membrane fouling (Mikkelsen 2001). The adsorption of individual EPS onto a gold surface was measured by QCM-D at a TOC concentration of 10 mg L^{-1} and the results ($n = 5$) are illustrated in Figure 3. The patterns of the frequency shift (Δf) and dissipation change (ΔD) with time of all the EPS solution were similar (Figure 3(a) and 3(b)). When the EPS was injected, Δf decreased, and ΔD increased from the baseline. The EPS enhanced deposition rate is represented by the higher frequency and dissipation shifts of the Au-coated crystal. Near steady-state, the values of Δf were about −5, −19.1 and −25.4 Hz for S-EPS, TB-EPS and LB-EPS samples, respectively, indicating that, of all the EPS fractions, LB-EPS had the highest adsorbed amount according to the Sauerbrey equation. The ΔD of S-EPS, LB-EPS and TB-EPS samples were 0.77×10^{-6}, 3.35×10^{-6} and 2.78×10^{-6}, respectively. The normalized dissipation, $\Delta D/\Delta f$, provides structural information of the adsorbed layer (Yan *et al.* 2011). Figure 3(c) presents the plots of ΔD against Δf for individual EPS at the fifth overtone. The $\Delta D/\Delta f$ slope was steepest for S-EPS layers, followed by TB-EPS layers and then LB-EPS layers, implying the conformations of the adsorbed layer for individual EPS were obviously different. A high $\Delta D/\Delta f$ ratio corresponds to a relatively nonrigid open structure, whereas a low ratio corresponds to a stiffer and more compact structure where the adsorbed mass induces relatively low energy dissipation(Yan *et al.* 2011). Therefore the adsorbed layer of LB-EPS has stiffer and more compact structure than that of S-EPS and TB-EPS in this study. A significant increase of the slope of $\Delta D/\Delta f$ for S-EPS was found when the Δf value was 4 Hz, indicating coverage-induced structural changes in the adsorbed layer, and the layer became more nonrigid and incompact due to the decreased packing density. The results of QCM-D clearly demonstrated that the LB-EPS has the highest adsorbed amount and the adsorbed layer of LB-EPS has stiffer and more compact structure, compared with the other fractions.

The characteristics of individual EPS

The general characteristics of individual EPS

The concentrations of S-EPS, LB-EPS and TB-EPS, indicated by the TOC, are shown in Table 1. It was noted that TB-EPS concentration (145 mg-TOC L^{-1}) in wastewater sludge was significantly higher than the concentration of LB-EPS and S-EPS (51.37 mg-TOC L^{-1} and 21.1 mg-TOC L^{-1}, respectively). UV_{254} is usually used to define the content of aromatic structures within the bulk dissolved organic matter samples and sludge organic matter (Her *et al.* 2003; Wei *et al.* 2011). Fractionation results (Table 1) indicated that TB-EPS had the predominant aromatic fraction of all the EPS fractions (accounted for 65.79% of all

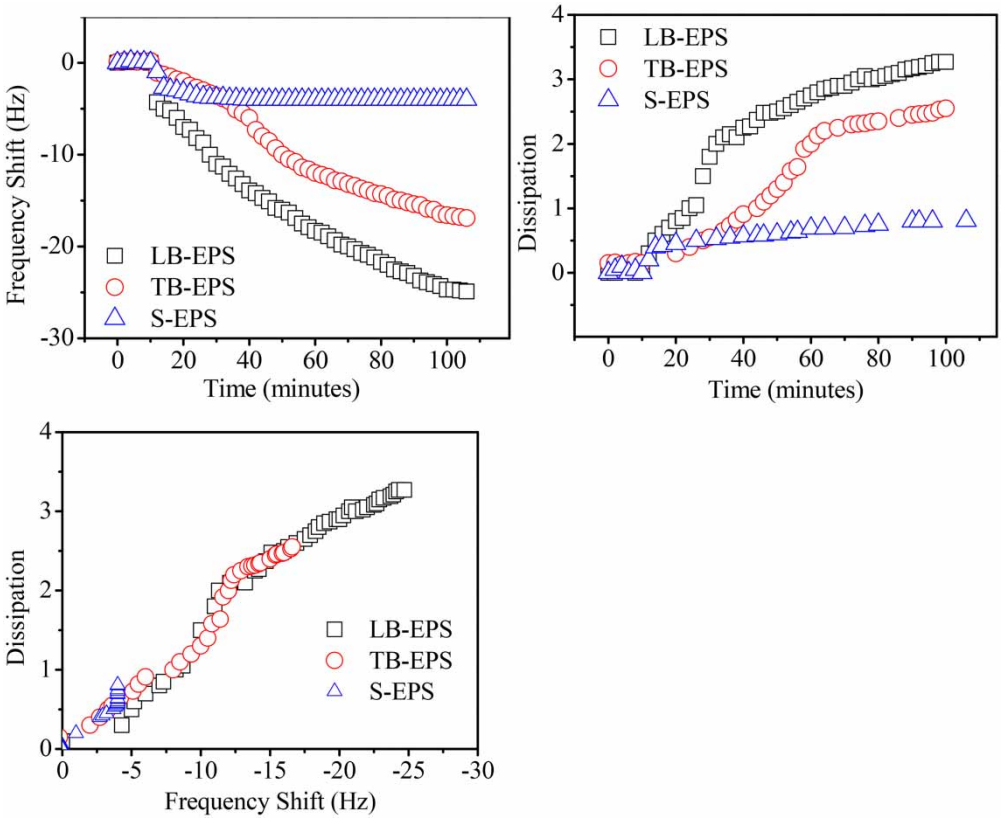

Figure 3 | Adsorption kinetic of individual EPS through QCM-D analysis at the fifth overtone.

Table 1 | Characteristics of individual EPS

Component	S-EPS	LB-EPS	TB-EPS
TOC (mg L^{-1})	21.1 ± 2.3	51.37 ± 5.6	145 ± 9.5
UV_{254} (m^{-1})	10.0 ± 1.4	49.8 ± 6.3	115.0 ± 12.1
SUVA (L m^{-1} mg^{-1})	0.47 ± 0.02	0.97 ± 0.05	0.79 ± 0.03

the EPS UV_{254}), followed by LB-EPS (28.49%) and S-EPS (5.72%). Furthermore, SUVA (L m^{-1} mg^{-1}) of individual EPS showed a decreasing trend: LB-EPS (0.97 L m^{-1} mg^{-1}) > TB-EPS (0.79 L m^{-1} mg^{-1}) > S-EPS (0.47 L m^{-1} mg^{-1}). SUVA is closely related to the aromaticity and/or hydrophobicity of the organic matter (Zhang *et al.* 2011). Relatively low SUVA value of the EPS (0.47–0.97 L m^{-1} mg^{-1}) implied the relatively low aromaticity and hydrophobicity of these EPS. The non-aromatic components of the EPS might be ascribed to the abundant existence of non-aromatic carbon chains, aliphatic carbon (fatty acids and polysaccharides) and fatty acids in the EPS. In this study, LB-EPS with a higher aromaticity and hydrophobicity showed more serious adsorptive fouling.

FTIR spectroscopic analysis

The FTIR spectra of LB-EPS, TB-EPS and S-EPS from the sewage sludge are illustrated in Figure 4 to detect the functional groups of individual EPS.

The transmittance of the TB-EPS and S-EPS spectra shows similar peaks. The spectra of TB-EPS shows a broad band at 3,700 cm^{-1}–3,300 cm^{-1}, attributed to O-H stretching in carboxylic functional groups and N-H stretching in amide functions (An *et al.* 2009). The band at 1,640 cm^{-1} was assigned to the stretching vibration of C = O and C-N in amide groups (amide 1), representing a typical characteristic of proteins. Moreover, the band at 1,384 cm^{-1} indicated the presence of lipids (Ramesh *et al.* 2006) in TB-EPS. The bands at 1,000–1,200 cm^{-1} can be assigned to C-O stretching, indicating the presence of carbohydrates or carbohydrates-like substances (An *et al.* 2009). The functional groups indicated by the sharp peak at 419, 619, 836, 873, 940 and 983 cm^{-1}, which belongs to the fingerprint region, could hardly be predicted; however, the fingerprint region of extracted EPS based on FTIR spectra may be used to discern different bacterial species (Wang

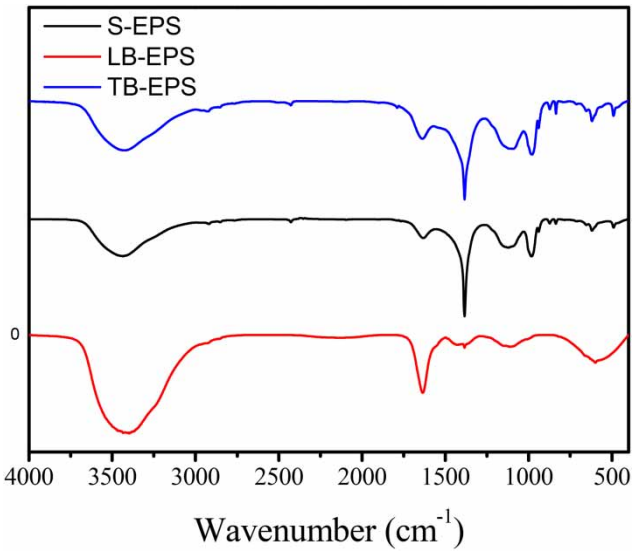

Figure 4 | FTIR spectra of individual EPS.

et al. 2009b), which is not discussed in this study. Based on the analysis above, TB-EPS and S-EPS samples mainly contained protein, carbohydrates and lipids.

In comparison with TB-EPS, the spectrum of LB-EPS shows similarities on the peaks of 3,700–3,300 cm^{-1}, 1,640 cm^{-1}, 1,425 cm^{-1}, 1,384 cm^{-1}, and 1,000–1,200 cm^{-1}, which demonstrates the presence of O-H bonds, proteins, phenolics, lipids, and carbohydrates in LB-EPS. Compared to S-EPS and TB-EPS, LB-EPS samples contained a larger amount of protein and less carbohydrates and lipids. However, it could be observed that the number of peaks in the LB-EPS spectrum is less than that of the TB-EPS and S-EPS spectrum especially between 500 cm^{-1} and 1,200 cm^{-1}, which illustrates the organic substances in TB-EPS and S-EPS were more complicated than those in LB-EPS.

EEM fluorescence analysis

The three-dimensional EEM fluorescence spectroscopy was applied to characterize the LB-EPS, TB-EPS and S-EPS (Figure 5). There were five principal EEM peaks (Regions I–V) based on different excitation/emission wavelengths (Ex/Em) by previous studies. The first and the second

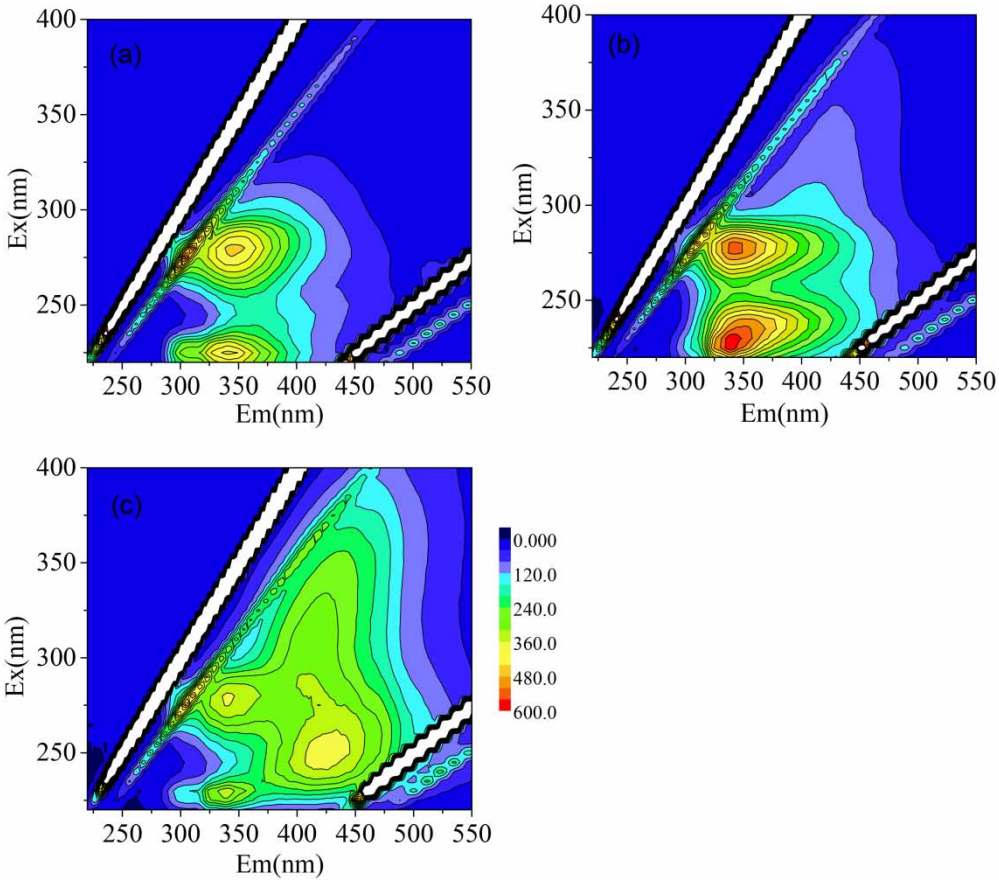

Figure 5 | Fluorescence EEMs for individual EPS: (a) TB-EPS, (b) LB-EPS and (c) S-EPS.

peak were aromatic protein-like substances I and II such as tyrosine and tryptophan (Ex/Em = 220–230/290–320 nm and Ex/Em = 220–240/320–360 nm). The third peak was fulvic acid-like materials (Ex/Em = 220–250/380–430 nm). The fourth peak was soluble microbial byproduct-like material (Ex/Em = 260–290/320–370 nm). The fifth peak was humic acid-like substance (Ex > 265 nm and Em > 380 nm) (Chen *et al.* 2003).

As revealed in Figure 5, two peaks were noticeable in all EEM spectra of EPS, whose main components were identified as tryptophan protein-like substances and soluble microbial byproduct-like material, respectively. Referring to S-EPS, it is evident that another two peaks (humic substance-like materials and fulvic acid-like materials) could also be readily identified from the EEM fluorescence spectra. Meanwhile, the LB-EPS fraction showed the highest fluorescent intensity in Region II and Region IV, demonstrating that the tryptophan protein-like substances and soluble microbial byproduct-like material in LB-EPS were the most abundant. This was in consistent with the results of FTIR.

In order to better understand the similarities and differences of individual EPS samples, the fluorescence regional integration (FRI) of each EEM region is summarized in Figure 6, which could be used for quantitative analysis (Chen *et al.* 2003). It can be seen that the FRI distribution of individual EPS varied widely. For LB-EPS, the FRI of Region I and Region II accounted for 23.48%; the corresponding FRI was 18.48% and 5.49% for TB-EPS and S-EPS, respectively. The LB-EPS had the highest FRI of Regions I and II of all. As mentioned above, Regions I and II are both related to protein-like substances and Region IV is related to soluble microbial byproduct-like material. It is well known that proteins play a crucial role in the structure, properties and functions of microbial aggregates (Wang *et al.* 2009a). The difference in protein composition should be well correlated with the functions that the individual EPS fraction played in sludge flocs and membrane fouling. Furthermore, the proteins adsorb much faster on membrane surfaces and are more difficult to remove than polysaccharides, playing an important role in initiating biofouling (Contreras *et al.* 2011). In this study, the LB-EPS contained a large amount of protein, especially aromatic proteins, compared to S-EPS and TB-EPS, and showed a higher aromaticity and hydrophobicity. These characteristics should be responsible for more severe fouling, and stiffer and more compact structure of the adsorbed layer.

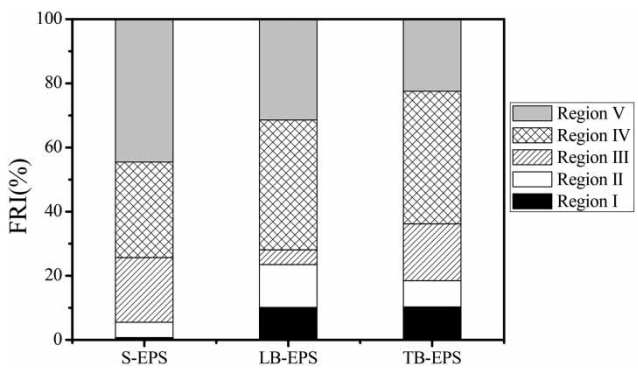

Figure 6 | FRI distribution of individual EPS.

CONCLUSION

The conclusions of this study can be summarized as follows.

(1) The significant adsorptive fouling only occurred in the initial hours. The degrees of adsorptive fouling for the three EPS fraction were in the order S-EPS < TB-EPS < LB-EPS. And the surface of membrane fouled by LB-EPS was rougher than that of the other EPS fractions.
(2) The LB-EPS had the highest adsorbed amount by QCM-D, and the adsorbed layer of LB-EPS had a stiffer and more compact structure, compared with the other EPS fractions.
(3) The LB-EPS contained a larger amount of protein (especially aromatic proteins), and less carbohydrates and lipids, exhibiting characteristics of greater aromaticity and hydrophobicity, compared with the other EPS fractions.

ACKNOWLEDGEMENTS

This study was supported by the National Natural Science Foundation of China (No. 51408169) and the Doctoral Scientific Research Foundation of Harbin University of Commerce (15KJ16).

REFERENCES

An, Y., Wang, Z., Wu, Z., Yang, D. & Zhou, Q. 2009 Characterization of membrane foulants in an anaerobic non-woven fabric membrane bioreactor for municipal wastewater treatment. *Chemical Engineering Journal* **155** (3), 709–715.

APHA 1995 *Standard Methods for the Examination of Water and Wastewater*. American Public Health Association/American

Water Works Association/Water Environment Federation, Washington, DC.

Boltz, J. P., Smets, B. F., Rittmann, B. E., van Loosdrecht, M. C. M., Morgenroth, E. & Daigger, G. T. 2017 From biofilm ecology to reactors: a focused review. *Water Science and Technology* **75** (8), 1753–1760.

Chen, W., Westerhoff, P., Leenheer, J. A. & Booksh, K. 2003 Fluorescence excitation-emission matrix regional integration to quantify spectra for dissolved organic matter. *Environmental Science & Technology* **37** (24), 5701–5710.

Contreras, A. E., Steiner, Z., Miao, J., Kasher, R. & Li, Q. 2011 Studying the role of common membrane surface functionalities on adsorption and cleaning of organic foulants using QCM-D. *Environmental Science & Technology* **45** (15), 6309–6315.

Deng, L., Guo, W., Ngo, H. H., Zhang, H., Wang, J., Li, J., Xia, S. & Wu, Y. 2016 Biofouling and control approaches in membrane bioreactors. *Bioresource Technology* **221**, 656–665.

Drews, A. 2010 Membrane fouling in membrane bioreactors—Characterisation, contradictions, cause and cures. *Journal of Membrane Science* **363** (1–2), 1–28.

Drews, A., Vocks, M., Iversen, V., Lesjean, B. & Kraume, M. 2006 Influence of unsteady membrane bioreactor operation on EPS formation and filtration resistance. *Desalination* **192** (1–3), 1–9.

Guo, W., Ngo, H.-H. & Li, J. 2012 A mini-review on membrane fouling. *Bioresource Technology* **122**, 27–34.

Her, N., Amy, G., McKnight, D., Sohn, J. & Yoon, Y. 2003 Characterization of DOM as a function of MW by fluorescence EEM and HPLC-SEC using UVA, DOC, and fluorescence detection. *Water Research* **37** (17), 4295–4303.

Herzberg, M., Kang, S. & Elimelech, M. 2009 Role of extracellular polymeric substances (EPS) in biofouling of reverse osmosis membranes. *Environmental Science & Technology* **43** (12), 4393–4398.

Kim, H. Y., Yeon, K. M., Lee, C. H., Lee, S. & Swaminathan, T. 2006 Biofilm structure and extracellular polymeric substances in low and high dissolved oxygen membrane bioreactors. *Separation Science and Technology* **41** (7), 1213–1230.

Kimura, K., Nishisako, R., Miyoshi, T., Shimada, R. & Watanabe, Y. 2008 Baffled membrane bioreactor (BMBR) for efficient nutrient removal from municipal wastewater. *Water Research* **42** (3), 625–632.

Le-Clech, P., Chen, V. & Fane, T. A. G. 2006 Fouling in membrane bioreactors used in wastewater treatment. *Journal of Membrane Science* **284** (1–2), 17–53.

Li, X. Y. & Yang, S. F. 2007 Influence of loosely bound extracellular polymeric substances (EPS) on the flocculation, sedimentation and dewaterability of activated sludge. *Water Research* **41** (5), 1022–1030.

Malamis, S. & Andreadakis, A. 2009 Fractionation of proteins and carbohydrates of extracellular polymeric substances in a membrane bioreactor system. *Bioresource Technology* **100** (13), 3350–3357.

Meng, F., Zhang, S., Oh, Y., Zhou, Z., Shin, H.-S. & Chae, S.-R. 2017 Fouling in membrane bioreactors: an updated review. *Water Research* **114**, 151–180.

Mikkelsen, L. H. 2001 The shear sensitivity of activated sludge: relations to filterability, rheology and surface chemistry. *Colloids and Surfaces A: Physicochemical and Engineering Aspects* **182** (1–3), 1–14.

Motsa, M. M., Mamba, B. B. & Verliefde, A. R. D. 2015 Combined colloidal and organic fouling of FO membranes: the influence of foulant-foulant interactions and ionic strength. *Journal of Membrane Science* **493**, 539–548.

Nagaoka, H., Ueda, S. & Miya, A. 1996 Influence of bacterial extracellular polymers on the membrane separation activated sludge process. *Water Science and Technology* **34** (9), 165–172.

Ognier, S., Wisniewski, C. & Grasmick, A. 2002 Membrane fouling during constant flux filtration in membrane bioreactors. *Membrane Technology* **2002** (7), 6–10.

Ramesh, A., Lee, D. J. & Hong, S. G. 2006 Soluble microbial products (SMP) and soluble extracellular polymeric substances (EPS) from wastewater sludge. *Applied Microbiology and Biotechnology* **73** (1), 219–225.

Rojas, M. E. H., Van Kaam, R., Schetrite, S. & Albasi, C. 2005 Role and variations of supernatant compounds in submerged membrane bioreactor fouling. *Desalination* **179** (1–3), 95–107.

Shen, Y. X., Zhao, W. T., Xiao, K. & Huang, X. 2010 A systematic insight into fouling propensity of soluble microbial products in membrane bioreactors based on hydrophobic interaction and size exclusion. *Journal of Membrane Science* **346** (1), 187–193.

Sheng, G. P., Yu, H. Q. & Li, X. Y. 2010 Extracellular polymeric substances (EPS) of microbial aggregates in biological wastewater treatment systems: a review. *Biotechnology Advances* **28** (6), 882–894.

Su, X., Tian, Y., Zuo, W., Zhang, J., Li, H. & Pan, X. 2014 Static adsorptive fouling of extracellular polymeric substances with different membrane materials. *Water Research* **50**, 267–277.

Sun, M., Wu, M., Liu, W., Liu, H., Zhang, Y. & Dai, J. 2016 3DEEM spectroscopy analysis to assess the EPS composition in different carriers in HMBR systems. *Water Science and Technology* **74** (11), 2708–2716.

Sweity, A., Ying, W., Ali-Shtaye, M. S., Yang, F., Bick, A., Oron, G. & Herzberg, M. 2011 Relation between EPS adherence, viscoelastic properties, and MBR operation: biofouling study with QCM-D. *Water Research* **45** (19), 6430–6440.

Wang, Z. W., Wu, Z. C. & Tang, S. J. 2009a Characterization of dissolved organic matter in a submerged membrane bioreactor by using three-dimensional excitation and emission matrix fluorescence spectroscopy. *Water Research* **43** (6), 1533–1540.

Wang, Z. W., Wu, Z. C. & Tang, S. J. 2009b Extracellular polymeric substances (EPS) properties and their effects on membrane fouling in a submerged membrane bioreactor. *Water Research* **43** (9), 2504–2512.

Wang, J., Wang, L., Miao, R., Lv, Y., Wang, X., Meng, X., Yang, R. & Zhang, X. 2016 Enhanced gypsum scaling by organic fouling layer on nanofiltration membrane: characteristics and mechanisms. *Water Research* **91**, 203–213.

Wei, L.-L., Zhao, Q.-L., Hu, K., Lee, D.-J., Xie, C.-M. & Jiang, J.-Q. 2011 Extracellular biological organic matters in sewage sludge during mesophilic digestion at reduced hydraulic retention time. *Water Research* **45** (3), 1472–1480.

Yan, M., Liu, C., Wang, D., Ni, J. & Cheng, J. 2011 Characterization of adsorption of humic acid onto alumina using quartz crystal microbalance with dissipation. *Langmuir* **27** (16), 9860–9865.

Yang, X. L., Song, H. L., Chen, M. & Cheng, B. 2011 Characterizing membrane foulants in MBR with addition of polyferric chloride to enhance phosphorus removal. *Bioresource Technology* **102** (20), 9490–9496.

Ying, W., Yang, F., Bick, A., Oron, G. & Herzberg, M. 2010 Extracellular polymeric substances (EPS) in a hybrid growth membrane bioreactor (HG-MBR): viscoelastic and adherence characteristics. *Environmental Science & Technology* **44** (22), 8636–8643.

Yu, G. H., He, P. J., Shao, L. M. & He, P. P. 2008 Stratification structure of sludge flocs with implications to dewaterability. *Environmental Science & Technology* **42** (21), 7944–7949.

Zhang, J., Chua, H. C., Zhou, J. & Fane, A. G. 2006 Factors affecting the membrane performance in submerged membrane bioreactors. *Journal of Membrane Science* **284** (1–2), 54–66.

Zhang, G. J., Ji, S. L., Gao, X. & Liu, Z. Z. 2008 Adsorptive fouling of extracellular polymeric substances with polymeric ultrafiltration membranes. *Journal of Membrane Science* **309** (1–2), 28–35.

Zhang, Y., Tian, J. Y., Nan, J., Gao, S. S., Liang, H., Wang, M. L. & Li, G. B. 2011 Effect of PAC addition on immersed ultrafiltration for the treatment of algal-rich water. *Journal of Hazardous Materials* **186** (2–3), 1415–1424.

First received 3 July 2017; accepted in revised form 10 January 2018. Available online 24 January 2018